Cause of inaccuracies in the Padé approximant of the Born series for strong electromagnetic scattering problems

J. B. P. de Graaff,[1,*] T. A. van der Sijs,[1] H. P. Urbach,[1] and O. El Gawhary[1,2]

[1]*Optics Research Cluster, Imaging Physics Department, Delft University of Technology, Van der Waalsweg 8, 2628 CH Delft, The Netherlands*

[2]*ASML Research Netherlands B.V., De Run 6501, 5504 DR Veldhoven, The Netherlands*

The Born series applied to the Lippmann-Schwinger equation is a straightforward method for solving optical scattering problems, which however diverges except for very weak scatterers. Replacing the Born series by Padé approximants is a solution of this problem. However, in some cases it is rather difficult to obtain an accurate Padé approximant. In this paper we aim to understand the cause by studying the scattering by a cylinder. We find that there is a strong connection between eigenvalues of the Lippmann-Schwinger operator that are close to the real axis, the occurrence of a near-resonance, and the problematic behavior of the Padé approximant. The determination of these eigenvalues provides a general method to obtain, for any given geometry, materials for which near-resonances occur.

I. INTRODUCTION

Inverse electromagnetic problems are key in modern technologies such as semiconductor manufacturing [1]. In the inverse problem, a (known) electromagnetic field is incident on an unknown object, and the resulting scattered field is measured in the far field. The main idea is that information about the object is now encoded in this scattered intensity. By using *a priori* knowledge on the laws of physics which describe the interaction, this information can, depending on the noise, to a certain extent be retrieved from the measurements.

The determination of the object usually involves many simulations using a *forward model*, in which the interaction of the electromagnetic field is modeled on a range of known objects and the scattered field is simulated. The object can then be updated at each iteration until the simulated scattered intensity is close enough to the actual measurements.

Many different solvers exist for the forward problem; notable examples include general numerical methods such as finite-element method and the finite difference time domain method (FDTD) [2]. For electromagnetic problems specifically, we also have integral equation based solvers such as described in for example [3–5]. Other methods exist for more specific objects, such as periodic structures. In this case we have the S- and T-matrix methods [6,7], and the rigorous coupled-wave analysis [8–10].

A disadvantage of the above methods is that they often require an iterative process to solve a large system of equations, making them computationally expensive. Another downside is that these numerical solvers lose the connection with the physical mechanisms that give the solution, since they function as a "black box" solver.

Hence it is often desirable to employ a more analytical approach to scattering problems. One way is to use the Born series solution of the Lippmann-Schwinger (LS) integral equation [11,12]. In the Born series approach, the solution is a power series, where the kth term represents the kth-order multiple scattering effect. Each term in the series is computed from the previous term through an application of an integral operator. The Born series converges for small permittivity contrast. In most practically relevant cases however, the Born series diverges.

A few methods have been proposed to mitigate this divergence; one example is the modified Born series [13,14], which changes the Green's function and the free-space permittivity by adding a small absorption to the background medium to make the Born series convergent for arbitrary permittivity contrasts. Another method is the Born-Padé method for optical scattering problems, as described in [15,16]. The Born-Padé method extends the applicability of the Born series by replacing it by rational functions derived thereof. These rational functions are called Padé approximants.

Apart from providing insight in multiple scattering processes, an advantage of this approach is that a close approximation to the solution of the scattering problem can be obtained with relatively few terms of the Born series, and that, in comparison with iterative methods, only a negligible amount of computer memory storage is needed. This makes the method suitable to applications in inverse imaging and metrology due to its speed. However, in some cases one has to use Born-Padé approximants of (very) high order to obtain sufficient accuracy. In this paper, we investigate the cause of this problem. We look at the behavior of the Born-Padé method for different materials (both dielectrics and metals) by computing the eigenvalues of the Green's integral operator of the LS equation. It turns out that when one of these eigenvalues is close to 1, the Padé approximant converges slowly and conversely.

---

*Contact author: J.B.P.deGraaff@tudelft.nl

As will be made clear, for any arbitrary geometry, the determination of eigenvalues which are close to the real axis of the LS operator with permittivity contrast of all scatterers chosen to be unity provides a general method for finding materials of the scatterers for which a near-resonance occurs. This is interesting to enhance sensitivity and resolution in sensing and imaging.

This paper is organized in the following way. In Sec. II, we give a brief derivation of the Born series for the two-dimensional (2D) optical scattering problem. In Sec. III we briefly explain the Born-Padé method in general terms. In Sec. IV we compute the spectrum of the scattering operator for the case of scattering by a cylinder, and make a link with the near-resonances of the scattering object. In Secs. V and VI we give some physical examples of the Born-Padé method at near-resonances, and compare the Born-Padé approach for different materials. Section VII contains a summary and conclusions.

II. THE BORN SERIES FOR THE LIPPMANN-SCHWINGER EQUATION

In this paper, we consider only two-dimensional scattering problems, however the theory generalizes to three-dimensional problems. We consider time-harmonic fields with frequency $\omega > 0$, so the time dependence is given by $\exp(-i\omega t)$. Let $k = 2\pi$ be the wave number in vacuum, where the unit of length is chosen such that the wavelength is unity. Let $\varepsilon_1 > 0$ be the real relative permittivity of the homogeneous medium which surrounds the scattering objects and let $n_1 = \sqrt{\varepsilon_1}$ be its refractive index. Although there may be several scattering objects, we assume for simplicity that there is only one object, which is invariant with respect to the z coordinate of a Cartesian coordinate system (x, y, z) and which has a cross section in the (x, y) plane denoted by Ω. This object has relative permittivity ε_2 and refractive index $n_2 = \sqrt{\varepsilon_2}$. The relative permittivity ε_2 can be complex with positive imaginary part, which because of the assumed implicit time dependence given by the factor $\exp(-i\omega t)$ corresponds to a medium with absorption. A medium which has a permittivity with negative imaginary part is an active medium in which electromagnetic energy is being generated. Such materials are not considered in this paper.

We consider the scattering by an incident TE-polarized field $\mathbf{E}^i(\mathbf{r}_\perp)$, where $\mathbf{r}_\perp = (x, y)$, hence the incident field is independent of z. The relative permittivity contrast $\Delta\varepsilon$ is given by

$$\Delta\varepsilon(\mathbf{r}_\perp) = (\varepsilon_2 - \varepsilon_1)1_\Omega(\mathbf{r}_\perp),$$

where 1_Ω is equal to 1 inside Ω, and zero outside Ω. From here on we will refer to the relative permittivity contrast as the permittivity contrast. Under these circumstances it follows from Maxwell's equations that the total electric field $\mathbf{E}$ depends only on $\mathbf{r}_\perp$ and has only a z component. Then Maxwell's equations are equivalent to the following problem for the z component E_z of the total electric field:

$$\nabla_\perp^2 E_z(\mathbf{r}_\perp) + k^2 \varepsilon_1 E_z(\mathbf{r}_\perp) = 0, \quad \mathbf{r}_\perp \text{ outside } \Omega, \quad (2.1)$$

$$\nabla_\perp^2 E_z(\mathbf{r}_\perp) + k^2 \varepsilon_2 E_z(\mathbf{r}_\perp) = 0, \quad \mathbf{r}_\perp \text{ inside } \Omega. \quad (2.2)$$

Furthermore, we have an outgoing radiation condition for the scattered field $E_z^s = E_z - E_z^i$:

$$\lim_{r \to \infty} r^{1/2}\left(\frac{\partial E_z^s}{\partial r} - ikn_1 E_z^s\right) = 0, \quad (2.3)$$

with $r = |\mathbf{r}_\perp|$. Since in this paper neither the geometry nor the field depends on z, we will from now on write $\mathbf{r}$ and ∇ instead of $\mathbf{r}_\perp$ and $\nabla_\perp$, respectively. We rewrite (2.1) and (2.2) as one equation:

$$\nabla^2 E_z + k^2(\varepsilon_1 + \Delta\varepsilon)E_z = 0. \quad (2.4)$$

Since $E_z = E_z^i + E_z^s$ and E_z^i satisfies the free-space Helmholtz equation, i.e., $\nabla^2 E_z^i + k^2 \varepsilon_1 E_z^i = 0$, (2.4) can be written as

$$\nabla^2 E_z^s + k^2(\varepsilon_1 + \Delta\varepsilon)E_z^s = -k^2 \Delta\varepsilon E_z^i. \quad (2.5)$$

We now define the LS integral operator by

$$T_{\Delta\varepsilon} U(\mathbf{r}) := k^2 \iint_\Omega G(\mathbf{r}, \mathbf{r}')\Delta\varepsilon(\mathbf{r}')U(\mathbf{r}')\, d\mathbf{r}', \quad (2.6)$$

with G the Green's function of the 2D Helmholtz operator $\nabla^2 + k^2$ given by

$$G(\mathbf{r}, \mathbf{r}') = \frac{i}{4}H_0^{(1)}(kn_1|\mathbf{r} - \mathbf{r}'|), \quad \mathbf{r}, \mathbf{r}' \text{ in } \mathbb{R}^2. \quad (2.7)$$

The integral operator $T_{\Delta\varepsilon}$ is an operator from the space $L^2(\Omega)$ of square integrable functions into itself. With this notation, (2.5) can be rewritten as an integral equation on Ω:

$$E_z(\mathbf{r}) - T_{\Delta\varepsilon} E_z(\mathbf{r}) = E_z^i(\mathbf{r}), \quad \mathbf{r} \text{ in } \Omega. \quad (2.8)$$

This is the LS integral equation which we will use in the rest of this paper. For passive materials, i.e., for materials of which $\text{Im}(\Delta\varepsilon) \geqslant 0$, it is known that for every incident field E_z^i there is a unique solution E_z of (2.8) (see for example Sec. 8 in [17]). Hence a perfect resonance, i.e., a nonzero solution of (2.8) without incidence field, does not exist for objects of bounded cross section embedded in a homogeneous medium. Incidentally, the same is true for three-dimensional scattering problems when all the scattering objects are bounded in three dimensions.

A formal solution for the field component E_z is given by the Born series (in operator theory known as the Neumann series):

$$E_z = (1 - T_{\Delta\varepsilon})^{-1} E_z^i = \sum_{n=0}^\infty T_{\Delta\varepsilon}^n E_z^i, \quad (2.9)$$

which converges provided $\|T_{\Delta\varepsilon}\| < 1$, where $\|T_{\Delta\varepsilon}\|$ is the operator norm of the LS operator.

III. PADÉ APPROXIMANTS OF THE BORN SERIES

When the operator norm $\|T_{\Delta\varepsilon}\| \geqslant 1$, the above Born series (2.9) does not converge. This is typically the case in optical scattering problems. The approach in [15] to replace the Born series by Padé approximants derived thereof is based on first introducing a (complex) perturbation parameter σ and considering instead of (2.8) the perturbed LS equation:

$$E_z^{(\sigma)} - \sigma T_{\Delta\varepsilon} E_z^{(\sigma)} = E_z^i. \quad (3.1)$$

Similarly to the above, the formal solution can be written as

$$E_z^{(\sigma)} = \sum_{n=0}^{\infty} \sigma^n T_{\Delta\varepsilon}^n E_z^i. \quad (3.2)$$

The solution (2.9) is obtained by setting $\sigma = 1$. The series (3.2) converges if $|\sigma| < 1/\|T_{\Delta\varepsilon}\|$.

The Padé approximant of order (N, N) is a rational function of σ which replaces this series and is valid also for σ beyond the radius of convergence $1/\|T_{\Delta\varepsilon}\|$ of the power series (3.2):

$$P_N^N(\sigma, \mathbf{r}) = \frac{A_0(\mathbf{r}) + A_1(\mathbf{r})\sigma + \ldots A_N(\mathbf{r})\sigma^N}{1 + B_1(\mathbf{r})\sigma + \ldots + B_N(\mathbf{r})\sigma^N}. \quad (3.3)$$

The coefficients $A_0, \ldots, A_N$ and $B_1, \ldots, B_N$ are derived by equating, for every $\mathbf{r}$, $P_N^N(\sigma, \mathbf{r})$ to the partial sum of the first $2N + 1$ terms of the power series (3.2) [15,18]. This is justified by the assumption that for σ smaller than the convergence radius of the power series, both the power series and the Padé approximants are valid approximations of the solution. After obtaining $P_N^N(\sigma, \mathbf{r})$ we choose $\sigma = 1$ and thereby obtain an approximation of the solution to scattering problem (2.1)–(2.3). Note that in this paper we only consider Padé approximants for which the orders of the polynomials in the numerator and denominator are the same.

The Born-Padé method works even in cases where we have a strong scatterer, and hence it "extends" the Born series to a larger class of permittivity contrasts. For a more detailed study we refer the reader to [15].

In some cases, the Padé approximants converge very slowly or do not converge to the solution at all. To investigate this phenomenon we study the eigenvalues and eigenfunctions of the LS operator. We will do this in the sections below.

IV. EIGENVALUES AND EIGENFUNCTIONS OF THE INTEGRAL OPERATOR

For a given permittivity contrast $\Delta\varepsilon$, let ζ be an eigenvalue of the operator $T_{\Delta\varepsilon}$ and let U be an eigenfield so that

$$\zeta U - T_{\Delta\varepsilon} U = 0. \quad (4.1)$$

The operator $T_{\Delta\epsilon}$ is a compact operator on $L^2(\Omega)$ (see for instance Sec. 3.6.2 in [19]), and hence it has discrete eigenvalues which each have at most a finite number of linearly independent eigenfields. Furthermore, the eigenvalues have a unique accumulation point at zero. Because the kernel (2.7) is a complex function, the LS operator is not Hermitian. Hence, its eigenvalues are complex.

We will assume from now that $n_1 = 1$ and that $\Delta\varepsilon$ is a constant. This simplifies the analysis but the conclusions drawn are generally valid. For a constant $\Delta\varepsilon$ we have

$$T_{\Delta\varepsilon} U = \Delta\varepsilon T_1 U,$$

where

$$T_1 U(\mathbf{r}) = k^2 \iint_\Omega G(\mathbf{r}, \mathbf{r}') U(\mathbf{r}') \, d\mathbf{r}'$$

is the operator for permittivity contrast $\Delta\varepsilon = 1$. Then (4.1) can be written as

$$\frac{\zeta}{\Delta\varepsilon} U - T_1 U = 0. \quad (4.2)$$

Hence if ζ is an eigenvalue of $T_{\Delta\varepsilon}$ then $\zeta/\Delta\varepsilon$ is an eigenvalue of T_1.

For a given shape of the scattering object it is thus sufficient to determine the eigenvalues and eigenfields of T_1. We do this for the case of a cylinder, because then all eigenvalues can be determined relatively easily and because it is plausible that the conclusions derived for the cylinder are generally valid.

Let ζ be an eigenvalue of T_1 for the cylinder with radius $r = a$ (with respect to the wavelength) and let U be an eigenfield:

$$\zeta U - T_1 U = 0. \quad (4.3)$$

Since (4.3) implies

$$U - T_{1/\zeta} U = 0. \quad (4.4)$$

It follows that U is a solution of the scattering problem (2.1)–(2.3) for the cylinder with permittivity contrast $1/\zeta$ and without incident field. Such a solution can only exist when the material in the cylinder is active, i.e., when $\text{Im}(\Delta\varepsilon) < 0$, or equivalently $\text{Im}(1 + 1/\zeta) < 0$. We conclude therefore that for all eigenvalues the following holds:

$$\text{Im}(\zeta) > 0. \quad (4.5)$$

The eigenvalue ζ and eigenfield U in (4.4) can be obtained by solving the scattering problem for the cylinder without incident field and with permittivity in the cylinder given by

$$\varepsilon_\zeta = 1 + \frac{1}{\zeta}. \quad (4.6)$$

The eigenvalue ζ can be determined from the equation derived from the requirement that the tangential field components have to be continuous on the boundary $r = a$ of the cylinder. It is found that ζ must be a solution of

$$J_m(kn_\zeta a)\left[\frac{m}{a}H_m^{(1)}(kn_1 a) - kn_1 H_{m+1}^{(1)}(kn_1 a)\right]$$
$$- H_m^{(1)}(kn_1 a)\left[\frac{m}{a}J_m(kn_\zeta a) - kn_\zeta J_{m+1}(kn_\zeta a)\right] = 0, \quad (4.7)$$

for some integer m, where $n_\zeta = \sqrt{\varepsilon_\zeta}$ and J_m is the Bessel function of order m and $H_m^{(1)}$ the Hankel function of the first kind of order m. The absolute value of the left-hand side of (4.7) is shown as function of complex ζ in Fig. 1 for $m = 4$.

An eigenfield corresponding to eigenvalue ζ satisfying (4.7) is given by

$$U(r, \varphi) = \begin{cases} H_m^{(1)}(kn_1 a)J_m(kn_\zeta r)e^{im\varphi}, & 0 \leqslant r < a, \\ J_m(kn_\zeta a)H_m^{(1)}(kn_1 r)e^{im\varphi}, & r \geqslant a, \end{cases} \quad (4.8)$$

and it is unique apart from multiplication by a constant. We plot the amplitude and phase of this eigenfunction in Fig. 2 for the case that the radius of the cylinder is 1, $m = -1$, and $\zeta = 0.3906 + 0.0546i$. The permittivity contrast which corresponds to the eigenvalue is $\Delta\varepsilon = 1 + 1/\zeta = 3.51 - 0.35i$.

We denote the set of all eigenvalues (the spectrum) of operator T_1 by $\Sigma(T_1)$. Once we have computed $\Sigma(T_1)$ for radius $a = 1$, we can obtain $\Sigma(T_{\Delta\varepsilon})$ for a different permittivity contrast by $\Sigma(T_{\Delta\varepsilon}) = \Delta\varepsilon \Sigma(T_1)$. The dependence of the eigenvalues on the radius is more complicated. To see how the eigenvalues change with radius, we plot the spectrum for
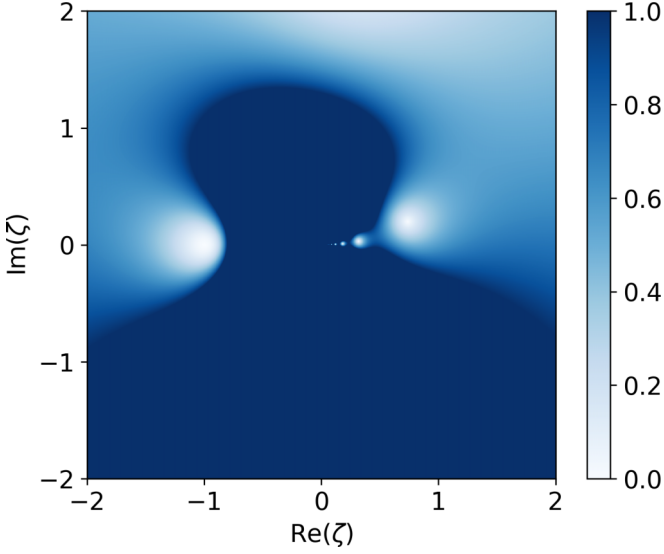
FIG. 1. A plot of the absolute value of (4.7) for $m = 4$, as a function of complex ζ. Even though not easily visible here, there is an infinite number of zeros approaching the origin.

FIG. 3. Visualization of the spectrum $\Sigma(T_1)$ in the complex plane for different values of the radius of the cylinder a. The number 1 is marked with a red cross.

$a = 0.5$, 1, 2, and 4. The results are shown in Fig. 3. As can be seen from the figure, all eigenvalues are in the upper half of the complex plane and approach zero, as should be. Furthermore, almost all eigenvalues have positive real part but a finite number of them have negative real part. We also see that the smallest distance of the eigenvalues to 1 decreases when the radius of the cylinder increases. This means that the norm of the resolvent operator $(I - T)^{-1}$ increases when the radius of the cylinder increases. This implies that the scattering problem for $\Delta\varepsilon = 1$ and large radius a has almost a resonance and that therefore the scattering problem is difficult to solve for this case.

For the above analysis we worked with a normalized permittivity contrast. In the next section we will consider the 2D cylinder with radius equal to the wavelength ($a = 1$), for both dielectrics and metals. Let us denote the smallest distance between the permittivity contrast and the reciprocals of the eigenvalues by
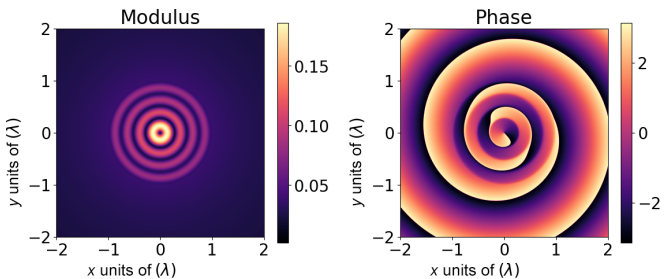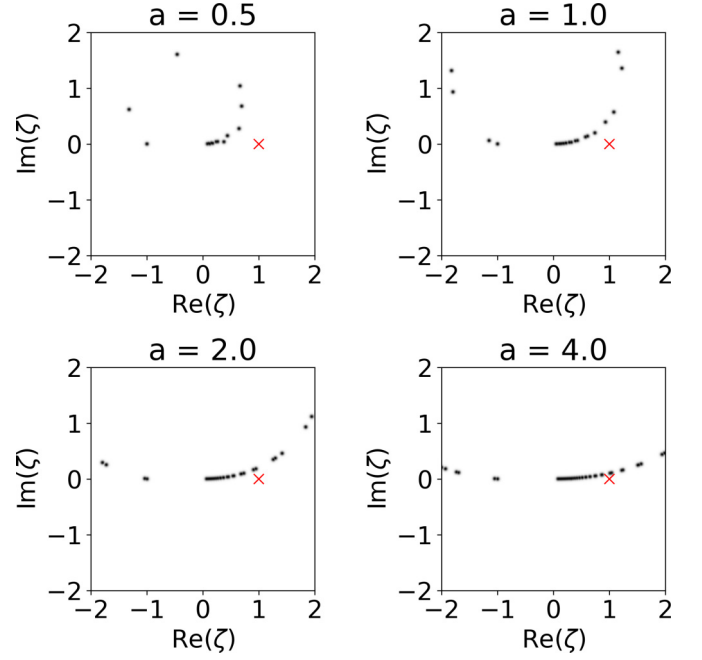
$$d(\Delta\varepsilon, \Sigma(T_1)^{-1}).$$

We will show that there is a connection between $d(\Delta\varepsilon, \Sigma(T_1)^{-1})$ and the rate of convergence for the Padé approximants.

V. PERFORMANCE OF THE PADÉ APPROXIMANTS UNDER VARYING CONDITIONS

In this section we consider the scattering by cylinders made of several materials. Let as before a be the radius of the cylinder and let $\Delta\varepsilon$ be the constant permittivity contrast. According to (3.1), the (unique) solution U of the scattering problem with incident field U^i satisfies

$$U(\mathbf{r}) - T_{\Delta\varepsilon}U(\mathbf{r}) = U^i(\mathbf{r}), \quad \text{for } \mathbf{r} \text{ in } \Omega, \quad (5.1)$$

or, equivalently,

$$\frac{1}{\Delta\varepsilon}U(\mathbf{r}) - T_1 U(\mathbf{r}) = \frac{1}{\Delta\varepsilon}U^i(\mathbf{r}). \quad (5.2)$$

For passive media, $\text{Im}(\Delta\varepsilon) \geqslant 0$ and hence $\text{Im}(1/\Delta\varepsilon) \leqslant 0$. Because all eigenvalues of T_1 have positive imaginary part, it follows that $1/\Delta\varepsilon$ is never equal to an eigenvalue of T_1. This agrees with the fact mentioned in Sec. II that the scattering problem (5.1) always has a unique solution. However, if one of the eigenvalues of T_1 has small imaginary part, then there can be passive materials whose permittivity contrast is close to the reciprocal of that eigenvalue. Then for that material the cylinder with the given radius has a near-resonance. As we will show, cases where the Padé approximant is inaccurate correspond one to one with cases where there is a near-resonance.

We consider the eigenvalue of T_1 equal to $\zeta = 0.0962 + 0.0030i$. Recall that this eigenvalue corresponds to a material
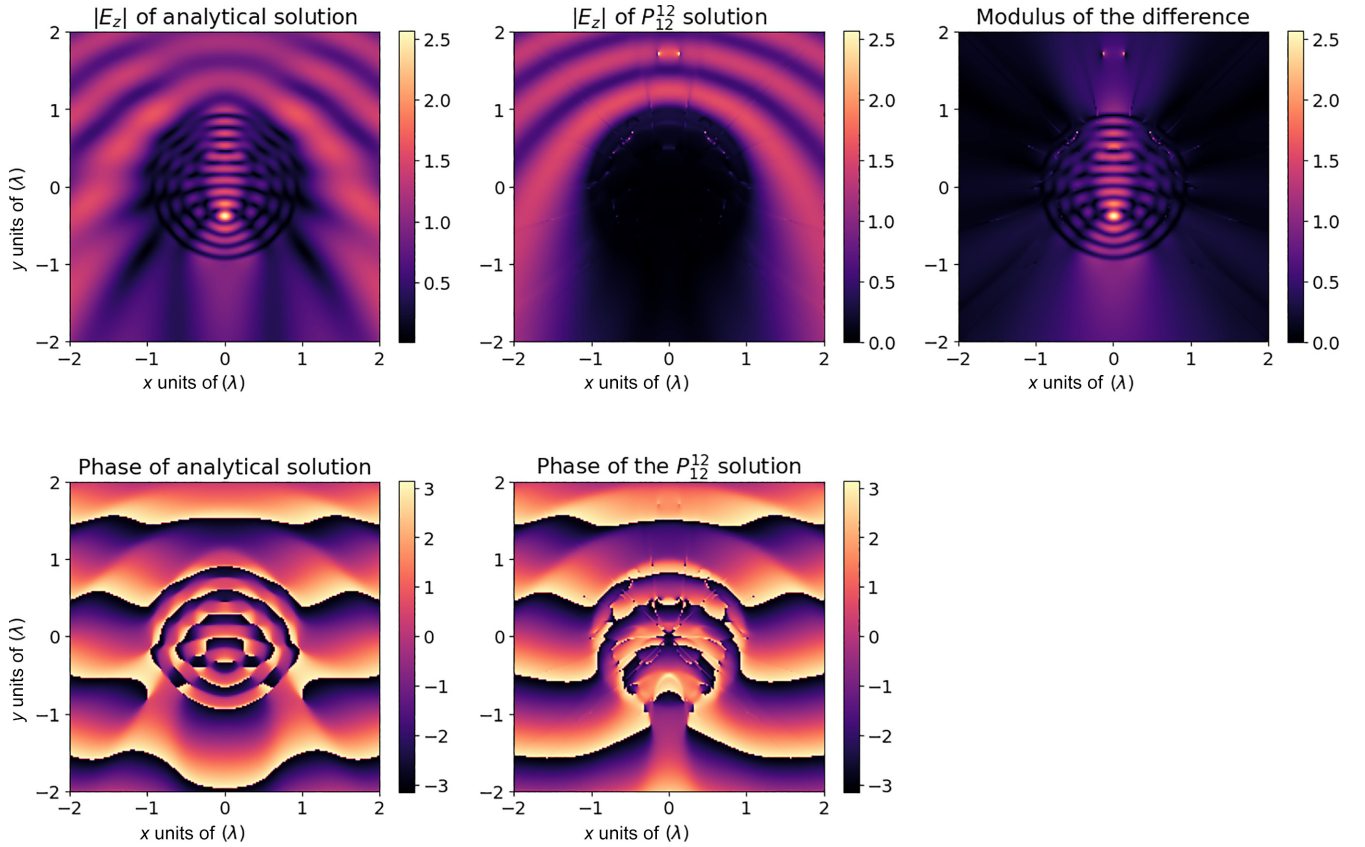

FIG. 2. Amplitude (left) and phase (right) of an eigenfunction U of T_1 for $a = 1$. This U belongs to eigenvalue $\zeta = 0.3906 + 0.0546i$ and $m = -1$.

FIG. 4. Comparison between $E_z(\mathbf{r})$ and $P_{12}^{12}(\mathbf{r})$ for $\Delta\varepsilon_r = 10.37 + 0.06i$ for a cylinder with radius $r = 1$, corresponding to GaP at a wavelength of 600 nm. The x axis and y axis are in units of wavelength.

with permittivity contrast given by

$$\Delta\varepsilon = 10.3747 - 0.3254i. \tag{5.3}$$

At a wavelength of 600 nm, gallium phosphide (GaP) has a permittivity $\varepsilon_2 = 11.37 + 0.06i$, giving a permittivity contrast of $\Delta\varepsilon = 10.37 + 0.06i$. The difference between this permittivity contrast and (5.3) is small.

We want to see how the Padé approximant behaves for the cylinder with permittivity contrast around this resonance permittivity contrast. We consider the scattering of an incident TE polarized plane wave which propagates in the positive y direction and has amplitude 1 when the cylinder has radius $a = 1$ and the permittivity contrast has real part equal to that of GaP and imaginary part varying between 0 and $+1$. For each permittivity contrast in this range, the analytical solution $E_z(\mathbf{r})$ and the Padé approximants $P_N^N(\mathbf{r})$ of the scattering problem for $N = 8, 10, 12$ are computed on the rectangle $D = [-2, +2]^2$. These are then compared using the relative L^2 error on D, i.e.,

$$e_N = \frac{\iint_D |E_z(\mathbf{r}) - P_N^N(\mathbf{r})|^2 \, d\mathbf{r}}{\iint_D |E_z(\mathbf{r})|^2 \, d\mathbf{r}}. $$

In Fig. 5 we see that the relative error is maximum for $\text{Im}(\Delta\varepsilon) = 0$ which corresponds to minimum distance to the eigenvalue.

In Fig. 4 we show the amplitude and phase of the Padé approximant P_{12}^{12} and the analytical solution when

$\Delta\varepsilon = 10.3747 + 0.06i$. Also the modulus of the difference of P_{12}^{12} and the analytical solution is shown. It is seen that for the relatively high value of $N = 12$, the solution is still not accurate.
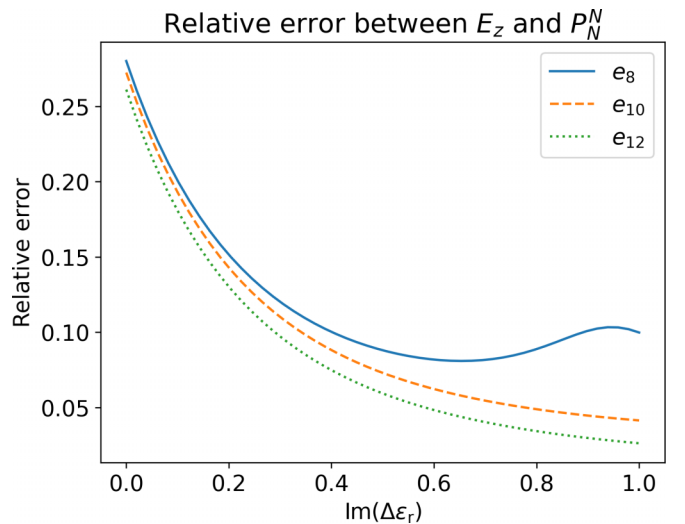

FIG. 5. Relative error of Padé approximants for varying the imaginary part of the permittivity contrast $\text{Im}(\Delta\varepsilon_r)$ from zero to $+i$. On the x axis is the imaginary part of the permittivity contrast, and on the y axis the relative error between E_z and P_N^N.
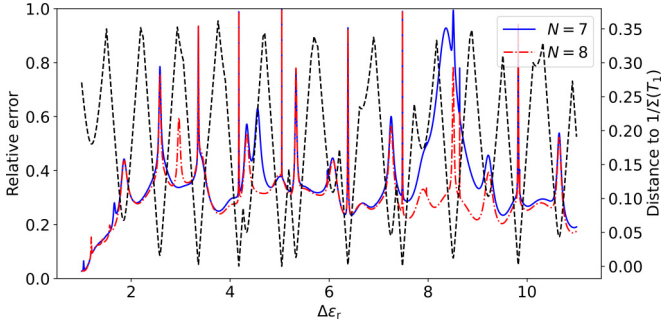
FIG. 6. Relative error of Padé approximants P_7^7 (blue solid line) and P_8^8 (red dash-dot line) for $1 < \Delta\varepsilon < 11$, and the distance of the $\Delta\varepsilon$ to the inverse of the spectrum of T_1 (dashed line).

We perform an analysis similar to Fig. 5, where we now consider purely real permittivities, with contrast varying from $\Delta\varepsilon_r = 1$ to 11. Permittivity contrasts with large real part and zero imaginary part can occur for example for silicon at terahertz wavelengths. Because $\Sigma(T_1)$ approaches zero close to the positive real axis, the reciprocals of the eigenvalues have large positive real part and small imaginary part. We expect this to cause problems for materials with high dielectric constant. In Fig. 6 we plot the accuracy of the Padé approximant P_7^7. As before, we consider for each $1 < \Delta\varepsilon < 11$ the logarithm of the L^2 difference between E_z and P_N^N, and also show the distance $d(\Delta\varepsilon, \Sigma(T_1)^{-1})$. It is seen that the largest inaccuracies of the Padé approximant correspond one to one with cases where the distance $d(\Delta\varepsilon, \Sigma(T_1)^{-1})$, i.e., the reciprocals of the eigenvalues are minimum (see Fig. 6).

To investigate the behavior of the Padé method for metals, we consider a cylinder made of silver (Ag) for different wavelengths. We vary the wavelength from 187 to 2066 nm, where in each step we change the permittivity of the cylinder. Since the cylinder has radius equal to the wavelength, the radius is changed together with the wavelength. Then the operator T_1 and hence the spectrum $\Sigma(T_1)$ remain the same. Now since the eigenvalues $\zeta \in \Sigma(T_1)$ accumulate to zero with positive imaginary part, the ζ^{-1} diverge to infinity with negative imaginary part. Hence, the distance between $\Delta\varepsilon$ and $1/\Sigma(T_1)$ grows as κ gets large. This can also be seen in the plots in Fig. 7.

This situation is interesting, since the modulus of the permittivity contrast is increasing with the wavelength, and hence $\|T_{\Delta\varepsilon}\|$ increases, but the distance $d(\Delta\varepsilon, \Sigma(T_1)^{-1})$ also grows.
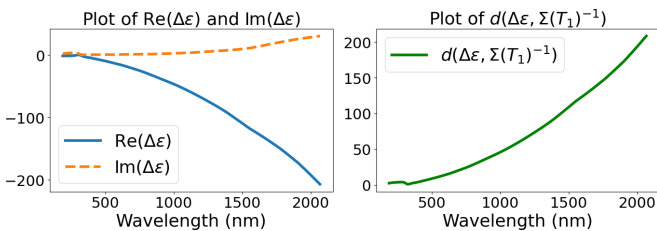

FIG. 7. Permittivity contrast for Ag at different wavelengths, and the minimum distance between the permittivity contrast and the reciprocals of the eigenvalues $\Sigma(T_1)$. Keeping the spectrum T_1 the same means that the radius is kept equal to the wavelength when the wavelength is varied.
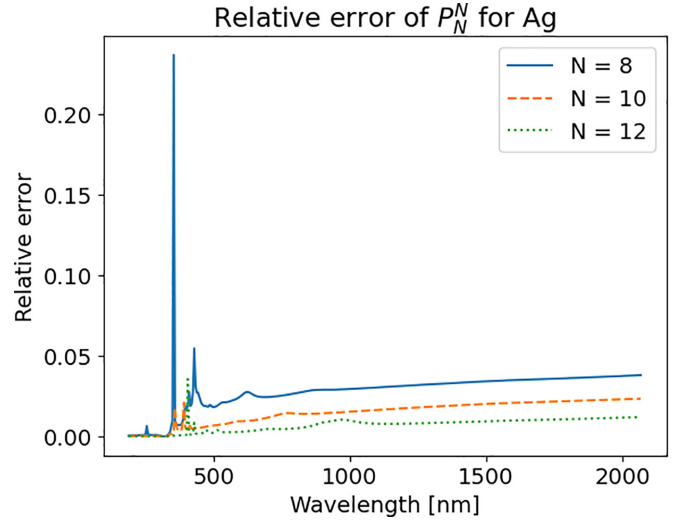

FIG. 8. Relative error of Padé approximants P_8^8, P_{10}^{10}, and P_{12}^{12} for Ag at different wavelengths. We see that the relative error stays below 5% at all wavelengths, except for a higher value reached around 352 nm for Padé order $N = 8$. Increasing the Padé order ($N = 10$ and 12, orange dashed curve and green dotted curve) removes this outlier.

In this case the Born series diverges wildly. The Padé approximant however, as we see in Fig. 8, still agrees with the analytical solution up to high precision: the relative error stays below 5%.

VI. RESONANCE PERMITTIVITIES FOR LARGER CYLINDERS

In the previous section, we have considered near-resonances for a cylinder with radius $a = 1$, i.e., the radius was equal to the wavelength. To get a better understanding on how the radius of the cylinder affects the eigenvalues of T_1, and thus the resonance permittivities, we look at a cylinder with radius $a = 2$ in this section.

We have seen in Fig. 3 that as the radius of the cylinder increases, the eigenvalues ζ in general have smaller imaginary part. Since the relation $\Delta\varepsilon = \zeta^{-1}$ holds, the permittivities associated with the ζ have a smaller negative imaginary part as well, and are thus closer to the real axis. So a strong near-resonance can now occur.

As an example of such a near-resonance, we consider the scattering of a TE polarized plane wave incident on a cylinder with radius $a = 2$. The relative permittivity corresponding to eigenvalue $\zeta = 0.15 + 6.2 \times 10^{-6}i$ is $\Delta\varepsilon = 6.31 - 2.4 \times 10^{-4}i$. We plot the result in the case where the permittivity of the cylinder is equal to $\Delta\varepsilon = 6.31$. This corresponds to a refractive index of $n = 2.704$ which is the refractive index of titanium dioxide (TiO_2) at a wavelength of 500 nm. The result is shown in Fig. 9.

To investigate the behavior of the Padé approximants on the cylinder with $a = 2$, a procedure similar to the one used to obtain Fig. 6 is used. For each $1 < \text{Re}(\Delta\varepsilon) < 11$, with $\text{Im}(\varepsilon) = 0$, the L^2 difference between the analytical solution E_z and the Padé approximant P_N^N are are shown in Fig. 10 for $N = 8$.
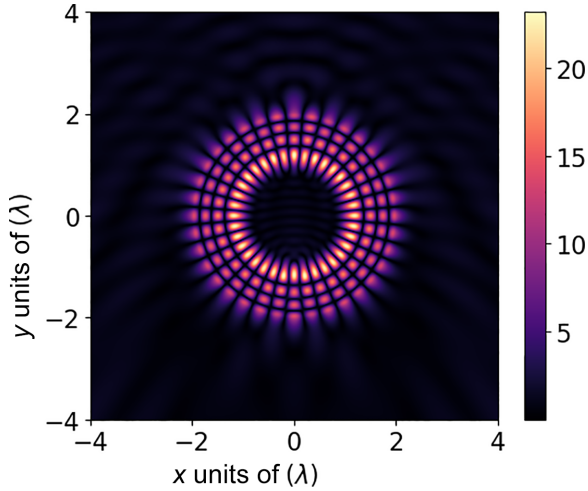
FIG. 9. The absolute value $|E_z|$ of the analytical solution of the scattering by a cylinder of a TE polarized plane wave of unit amplitude and incident in the positive y direction. The material is TiO$_2$, the wavelength is 500 nm for which the permittivity contrast is $\Delta\varepsilon = 6.31$, and the radius of the cylinder is twice the wavelength. This is a case where there is a near-resonance. Both axes are in units of the wavelength. A maximum field strength of $\approx 23\times$ the amplitude of the incidence plane wave is obtained inside the cylinder.

As expected, there are now more eigenvalues close to the real axis in this range, causing a lot of inaccurate Padé approximants. There is again a clear correspondence between the maxima of the log-L^2 difference and the minima of $d(\Delta\varepsilon, \Sigma(T_1)^{-1})$.

VII. CONCLUSIONS

In this paper, the cause of inaccuracies in the Born-Padé method was explained by considering the eigenvalues of the Lippmann-Schwinger integral operator T_1. For the cylinder we have analytically computed the eigenvalues of the operator with unit permittivity contrast T_1, and we have linked these to the permittivity contrasts for which optical resonances occur. These permittivities have however negative imaginary part and hence correspond to active materials. We demonstrated that if the permittivity contrast is close to the reciprocal of one of the eigenvalues of operator T_1, the scattering problem has an almost resonance and that then the Padé approximant is inaccurate. Furthermore, we considered three materials: GaP in visible wavelength range, a dielectric material with permittivity contrast ranging from $\Delta\varepsilon = 1$ to 11, and an Ag cylinder over a range of wavelengths. In this last case we looked at the convergence of P_8^8, P_{10}^{10}, and P_{12}^{12}. We have seen
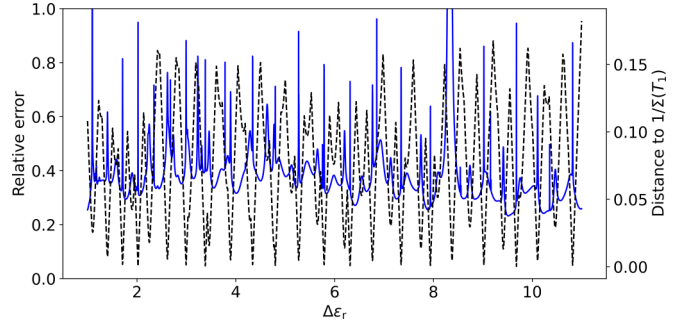

FIG. 10. A plot of the relative L^2 errors of the Padé approximant P_8^8 for $\Delta\varepsilon$ ranging from $+1$ to $+11$, for the cylinder with radius $a = 2$ (blue line). Furthermore, also the distance of $\Delta\varepsilon$ to the reciprocals of the points in the spectrum $\Sigma(T_1)$ is shown (black dashed line).

that Padé method works here even though the norm $\|T_{\Delta\varepsilon}\|$ is very large. In spite of this large norm, the reciprocal of the permittivity contrast of the metal is far from the spectrum of operator T_1, and the Padé approximant is accurate.

In conclusion, we have seen that the Born-Padé method works even for very strong scattering objects, as long as we stay sufficiently far away from the resonance permittivities. We found for the case of a homogeneous cylinder that when the Padé approximant is not accurate, the reciprocal of the permittivity contrast is close to an eigenvalue of the LS operator with unit permittivity contrast (T_1) and conversely, if there is an eigenvalue of T_1 which is close to the reciprocal of the permittivity contrast so that a near-resonance condition applies, the Padé approximant is inaccurate. When the scattering object is larger (radius of the cylinder is larger), T_1 has more eigenvalues close to the real axis and hence there is more permittivity contrast for which the Padé approximant converges slowly. It should be mentioned that when a near-resonance occurs, the scattering problem is more difficult to solve not only for the Padé method but for any numerical method (see for example [20] for the FDTD method, and [21,22] for the volume integral method).

Finally, we remark that the spectral analysis of the LS operator can be used to construct a near-resonance of objects with size of the order of the wavelength. In fact, if a is a typical length of the object, we choose a/λ between 1 and 3 say. Then we determine the eigenvalues of the operator T_1, for the given λ and a, which are close to the real axis. Then by choosing a material and a wavelength for which the relative permittivity contrast is close to the reciprocal of such an eigenvalue we obtain a resonance for this configuration. Note that since a/λ was chosen, finding an appropriate material and wavelength implies that the size of the object has to be adopted.

[1] C. J. Raymond, Scatterometry for semiconductor metrology, in *Handbook of Silicon Semiconductor Metrology*, edited by A. C. Diebold (CRC, Boca Raton, 2001), pp. 389–418.

[2] K. S. Yee, J. S. Chen, and A. H. Chang, Conformal finite difference time domain (FDTD) with overlapping grids, in *IEEE Antennas And Propagation Society International Symposium 1992 Digest* (Springer, New York, 1992), pp. 1949–1952.

[3] G. Vainikko, Fast solvers of the Lippmann-Schwinger equation, in *Direct and Inverse Problems of Mathematical Physics* (Springer, Boston, 2000), pp. 423–440.

[4] M. C. van Beurden, A spectral volume integral equation method for arbitrary Bi-periodic gratings with explicit Fourier factorization, Prog. Electromagn. Res. B **36**, 133 (2012).

[5] P. M. Van den Berg, *Forward and Inverse Scattering Algorithms Based on Contrast Source Integral Equations* (Wiley, New York, 2021).

[6] Z. Li and L. Lin, Photonic band structures solved by a plane-wave-based transfer-matrix method, Phys. Rev. E **67**, 046607 (2003).

[7] R. C. Rumpf, Improved formulation of scattering matrices for semi-analytical methods that is consistent with convention, Prog. Electromagn. Res. B **35**, 241 (2011).

[8] L. Li, Reformulation of the Fourier modal method for surface-relief gratings made with anisotropic materials, J. Mod. Opt. **45**, 1313 (1998).

[9] M. G. Moharam and T. K. Gaylord, Rigorous coupled-wave analysis of planar-grating diffraction, J. Opt. Soc. Am. **71**, 811 (1981).

[10] M. G. Moharam, E. B. Grann, D. A. Pommet, and T. K. Gaylord, Formulation for stable and efficient implementation of the rigorous coupled-wave analysis of binary gratings, J. Opt. Soc. Am. A **12**, 1068 (1995).

[11] M. Born and E. Wolf, *Principles of Optics: Electromagnetic Theory of Propagation, Interference and Diffraction of Light* (Elsevier, Amsterdam, 2013).

[12] L. Novotny and B. Hecht, *Principles of Nano-Optics* (Cambridge University Press, New York, 2012).

[13] G. Osnabrugge, S. Leedumrongwatthanakun, and I. M. Vellekoop, A convergent Born series for solving the inhomogeneous Helmholtz equation in arbitrarily large media, J. Comput. Phys. **322**, 113 (2016).

[14] T. Vettenburg, S. A. R. Horsley, and J. Bertolotti, Calculating coherent light-wave propagation in large heterogeneous media, Opt. Express **27**, 11946 (2019).

[15] T. A. van der Sijs, O. El Gawhary, and H. P. Urbach, Electromagnetic scattering beyond the weak regime: Solving the problem of divergent Born perturbation series by Padé approximants, Phys. Rev. Res. **2**, 013308 (2020).

[16] T. A. van der Sijs, O. El Gawhary, and H. P. Urbach, Padé approximants of the Born series of electromagnetic scattering by a diffraction grating, Phys. Rev. A **109**, 033522 (2024).

[17] D. L. Colton, R. Kress, and R. Kress, *Inverse Acoustic and Electromagnetic Scattering Theory* (Springer, New York, 1998).

[18] C. M. Bender and S. A. Orszag, *Advanced Mathematical Methods for Scientists and Engineers I: Asymptotic Methods and Perturbation Theory* (Springer, New York, 2013).

[19] G. W. Hanson and A. B. Yakovlev, *Operator Theory for Electromagnetics: An Introduction* (Springer, New York, 2013).

[20] P. H. Harms, J. F. Lee, and R. Mittra, A study of the nonorthogonal FDTD method versus the conventional FDTD technique for computing resonant frequencies of cylindrical cavities, IEEE Trans. Microwave Theory Tech. **40**, 741 (1992).

[21] A. Hoekstra, J. Rahola, and P. Sloot, Accuracy of internal fields in volume integral equation simulations of light scattering, Appl. Opt. **37**, 8482 (1998).

[22] J. Rahola, On the eigenvalues of the volume integral operator of electromagnetic scattering, SIAM J. Sci. Comput. **21**, 1740 (2000).